Journal of Statistical Physics, Vol. 104, Nos. 5/6, September 2001 (© 2001)

Crossing the Coexistence Line at Constant Magnetization

Michel Pleimling[1, 2] and Alfred Hüller[1]

Received March 18, 2001; revised April 24, 2001

Using Monte Carlo histogram methods, the microcanonical caloric curve is computed for the Ising model in two and three dimensions with fixed magnetization. Whereas the signatures of a possible first order phase transition are clearly visible for large systems, intriguing finite size effects are revealed for smaller system sizes. The behaviour of the caloric curve is studied in a systematic way. Furthermore, results for the thermal stability of three-dimensional droplets of minority spins inside the two-phase region are presented. The effect of the percolation transition on the stability of these droplets is discussed.

KEY WORDS: Ising model with fixed magnetization; coexistence line; microcanonical caloric curve; Monte Carlo simulation.

1. INTRODUCTION

The celebrated Ising model has in the past been studied extensively, mainly because of its conceptual simplicity in combination with non-trivial features and because of the fact that, in two dimensions, exact results can be obtained.[(1)] Besides being the best studied model in the theory of critical phenomena, it is for example also discussed in connection with magnetism, surface physics, or even nuclear physics (see ref. 2 for a recent overview on the use of classical microscopic models in nuclear physics).

In the present work we want to focus on the behavior of the two- and three-dimensional nearest neighbour Ising models inside the coexistence region. In the temperature-magnetization space this two-phase region is

[1] Institut für Theoretische Physik 1, Friedrich-Alexander-Universität Erlangen-Nürnberg, Staudtstraße 7, D-91058 Erlangen, Germany.

[2] Laboratoire de Physique des Matériaux, Laboratoire associé au CNRS UMR 7556, Université Henri Poincaré Nancy I, B.P. 239, F-54506 Vandœuvre lès Nancy Cedex, France.

0022-4715/01/0900-0971$19.50/0

bordered by the line of spontaneous magnetization, the coexistence line. Investigations inside the two-phase region mainly deal with non-equilibrium dynamics[3, 4] (analyzing, for example, the time evolution when the external field is switched or when the system is quenched from high temperatures) or with the equilibrium shape of droplets of minority spins.[5–7] Using Monte Carlo techniques we study the Ising model in the temperature-magnetization and in the energy-magnetization space when the magnetization density m is fixed at some value m_0. This approach has the advantage that data both below and above the coexistence line can be gathered without having to deal with the complications of an external field changing sign at the coexistence line.

Recently, properties of a surface with a constant coverage of adatoms have been described within a model equivalent to the two-dimensional Ising model with fixed magnetization (IMFM).[8] The transition between a cluster of monoatomic height at low temperatures and a gas of adatoms at higher temperatures, observed in that study, has led to a subsequent work on the two-dimensional IMFM where the finite-size dependences of the stability of minority clusters in small systems were elucidated.[11] These systems are small in comparison with the asymptotically large systems where rigorous results are available.[6, 7, 9, 10] In particular, numerical simulations of systems of finite size showed that the macroscopic droplets of minority spins (i.e., clusters whose radii scale with the system size) which disappear at the coexistence line in the thermodynamic limit, do that with the signatures of a possible phase transition as, e.g., pronounced maxima in cluster and thermal properties. In three dimensions, the IMFM model was considered in relation to nuclear matter fragmentation.[12] Here, based on simulations of moderate sized systems, the cluster transition was discussed in terms of a continuous transition taking place at the coexistence line. To be complete, we should also mention a recent study of the three-dimensional IMFM at the critical temperature.[13]

Based on general considerations on the topology of the entropy of finite systems,[14] one would expect to observe the finite-size signatures of a discontinuous transition when crossing this line at fixed magnetization, but recent numerical studies of finite systems in two[11] and three[12] dimensions seemed to be more compatibel with a continuous transition. Our main subject will be the microcanonical caloric curve as obtained from Monte Carlo simulations of the IMFM in two and three dimensions (analysing a vast range of different lattice sizes). Indeed, a thorough analysis of the caloric curve is expected to provide new insights. Furthermore, as a complement to ref. 11, we will also discuss the influence of finite-size effects on the thermal stability of macroscopic droplets of minority spins in three dimensions.

The paper is organized as follows. In the next section our simulation techniques are introduced. Especially, we want to point out how histogram methods can be used for the computation of the caloric curve. In Section 3, microcanonical caloric curves of the IMFM in two and three dimensions are discussed in detail, whereas the thermal stabilty of three-dimensional extensive droplets on finite lattices is investigated in Section 4. Finally, Section 5 gives our conclusions.

2. METHOD

Monte Carlo (MC) calculations have been developed into a universally applicable tool for problems which defy an exact solution by analytical methods. In statistical mechanics many of these extremely difficult problems occur in the vicinity of phase transitions. There the MC method serves the purpose of calculating the mean values of physically interesting quantities as, e.g., the energy density or the magnetization density of the system. The dissipation fluctuation theorem relates the response functions to the mean values of the spontaneous fluctuations of the corresponding densities. For the examples mentioned above the fluctuations yield the specific heat and the magnetic susceptibility, respectively.

The main purpose of MC calculations is thus the determination of mean values of densities and of their fluctuations.

Most calculations are performed for the experimentally relevant situation where the system of interest is in contact with a thermostat. There the microstates μ of the system appear according to the canonical distribution

$$p_\mu = \frac{\exp(-\beta E_\mu)}{Z} \tag{2.1}$$

where E_μ is the value of the energy in the microstate μ, β is the inverse temperature of the thermostat and Z the partition function

$$Z = \sum_\mu \exp(-\beta E_\mu). \tag{2.2}$$

In conventional MC calculations an approximation for the mean value of the energy

$$\langle E \rangle = \sum_\mu p_\mu E_\mu \tag{2.3}$$

is directly obtained in the course of the MC run by sampling the energy values E_t at v sufficiently distant instants t of the calculation

$$\langle E \rangle \cong \frac{1}{v} \sum_t E_t. \tag{2.4}$$

The mean value of the fluctuations are obtained by summing the equivalent expression for $\langle (E - \langle E \rangle)^2 \rangle$.

In recent years, however, the direct summation has frequently been replaced by the histogram method.[15] There one tries to find an approximation for the degeneracy $g(E_i)$ of the energy levels E_i of the system

$$g(E_i) = \sum_\mu \delta_{E_i, E_\mu}. \tag{2.5}$$

To this end the energy values E_t at the instants t are collected into a histogram:

$$g(E_i) \exp(-\beta E_i) = K \sum_t \delta_{E_i, E_t}. \tag{2.6}$$

Eq. (2.6) can be solved for $g(E_i)$ in the energy range where the statistical errors on the right hand side are sufficiently small. K is an undetermined constant.

Nothing is lost when a histogram is stored instead of the mean values. On the contrary there are several advantages: (1) Once $g(E_i)$ has been established, the canonical mean value of any function $X(E)$ of the energy can easily be calculated afterwards:

$$\langle X \rangle_{\beta'} = \sum_i g(E_i) \exp(-\beta' E_i)\, X(E_i)/Q_c \tag{2.7}$$

with

$$Q_c = \sum_i g(E_i) \exp(-\beta' E_i). \tag{2.8}$$

(2) As indicated by the prime in the formula (2.7), β' may deviate by a small amount from the value of β which has been used in the simulation where $g(E_i)$ was established. This allows the determination of the temperature dependence of $\langle X \rangle$ in a small range around $T = 1/\beta$. (3) With an algorithm that finds the best values for the undetermined constants K, histograms of MC runs at several temperatures may be combined to yield a

single broad histogam which may then be used to find the temperature dependence of $\langle X \rangle$ over the desired range.[15]

Here we shall exploit yet another advantage of the histogram method. (4) From the entropy $S(E) = \ln g(E)$ and the microcanonical definition

$$\beta^*(E) = \mathrm{d}S(E)/\mathrm{d}E \tag{2.9}$$

one finds the microcanonical inverse temperature β^*. For a finite system a plot of E versus $1/\beta^*(E)$ (the microcanonical caloric curve) shows a lot more detail than the equivalent canonical plot of $\langle E \rangle$ as a function of T. The sum in (2.3) involves an average over many energy levels, whereas (2.9) exhibits local anomalies of the density of states. There is furthermore no need to determine the constants K of MC runs at different temperatures. These drop out when the derivative is performed in (2.9). The bits of the E versus $1/\beta^*$ curve from the different runs join smoothly without any further need for adjustment.

Here we consider two and three dimensional Ising systems with ferromagnetic nearest neighbour interactions. The natural variables of the entropy are the energy E and the magnetization M. We are interested in the thermal behavior of a system with clamped magnetization $M = M_0$, which can be deduced from $g(E, M_0)$, the degeneracy of the states with fixed magnetization as a function of the energy. Fixing the magnetization means fixing the number of minority spins. At low energies almost all the minority spins form one big droplet whereas at high energies one observes a large number of small droplets composed of only a few minority spins.

In order to find $g(E, M_0)$ we perform a conventional canonical MC run at a temperature $T = 1/\beta$. At the start the system is prepared in any one of the states with $M = M_0$ and with an arbitrary energy E_i. During the procedure we randomly select one spin in the system and try to flip it. The flip leads to a new state with energy E' and magnetization M'. The flip is not performed if $M' > M_0 + 2$ or if $M' < M_0 - 2$. If M' is equal to one of the three admitted values M_0, $M_0 \pm 2$ of the magnetization, the spin is flipped with probability 1 if $E' \leqslant E_i$, and it is flipped with probability $\exp(\beta(E_i - E'))$ if $E' > E_i$. After every 1000 attempted spin flips a histogram $h(E, M)$ is augmented by 1 count at the actual value of E and M. This way one obtains estimators for $g(E, M) \exp(-\beta E)$ for the three allowed values of the magnetization and for a range of energies centered around $\langle E \rangle_\beta$ (2.7). Alternatively, one might have used Kawasaki dynamics, but our approach has the advantage that three histograms for the three allowed values of the magnetization are obtained in one run.

The degeneracy $g(E, M_0)$ can now be exploited in different ways. One can, e.g., calculate $\langle X \rangle$ from (2.7). For large enough systems this corresponds to a sampling of $X(E)$ with a gaussian distribution function centered at the most probable value of E which solves $\mathrm{d}S(E, M_0)/\mathrm{d}E|_{\tilde{E}} = \beta$. The width of the distribution

$$\Gamma_{\mathrm{can}} = (\mathrm{d}^2 S(E, M_0)/\mathrm{d}E^2)^{-\frac{1}{2}} \tag{2.10}$$

depends on the number N of spins in the system, but it tends to a constant for large system sizes. On the extensive energy scale $X(E)$ is therefore sampled over a constant range ΔE of energies and the relative width of the distribution $\Delta E/E_{\max}$ with $E_{\max} = dN$ (d being the dimensionality of the lattice) tends to zero with increasing system size.

One may also calculate local derivatives of $S(E, M_0)$ as, e.g., the microcanonically defined temperature $\beta^*(E, M_0) = S'(E, M_0) = \mathrm{d}S(E, M_0)/\mathrm{d}E$ or its derivative $\mathrm{d}\beta^*(E, M_0)/\mathrm{d}E = S''(E, M_0) = \mathrm{d}^2 S(E, M_0)/\mathrm{d}E^2$ which serve in the definition of the specific heat:

$$C(E) = -S'(E, M_0)^2/S''(E, M_0). \tag{2.11}$$

Statistical errors in the numericaly determined histogram $g(E, M_0)$ are unavoidable. These are accentuated when derivatives are formed. The fluctuations of $S'(E, M_0)$ and $S''(E, M_0)$ can be smoothed by gaussian sampling:

$$\{S'(E, M_0)\} = \sum_i S'(E_i, M_0) \exp(-(E_i - E)^2/(2\Gamma^2))/Q_m \tag{2.12}$$

where

$$Q_m = \sum_i \exp(-(E_i - E)^2/(2\Gamma^2)) \tag{2.13}$$

is the normalization. Equations (2.12) and (2.13) bear some resemblence with the canonical mean values of (2.7) and (2.8), but here we have the advantage that the center E and the width Γ of the gaussian distribution can be chosen at will - as long as the sampling is restricted to energy levels E_i with sufficiently accurate data.

The freedom of choosing the width Γ is exploited in a compromise between the demand of exhibiting the local anomalies of the entropy clearly and the goal of getting rid of the statistical errors as well as possible. Gaussian smoothing has the definite advantage over any other smoothing procedure that it does not create any spurious features which were not

present in the original data. In the canonical averaging procedure (2.7) Γ_{can} (see (2.10)) is fixed. The value of Γ in (2.13) should be as small as possible, but this depends on the quality of the data. In the examples of the next section we were able to keep Γ two orders of magnitude smaller than Γ_{can}. Therefore much finer details of the caloric curve can be resolved.

Besides using the procedure just described, we also simulated the IMFM model with an adapted nonlocal spin-exchange algorithm,[16] especially designed for the investigations of equilibrium crystal shapes, in order to study the thermal stability of extensive macroscopic droplets in three dimensions.

3. THE CALORIC CURVE

Recently, the thermal stability of macroscopic droplets of minority spins in small systems has been investigated at fixed magnetization in the two-dimensional Ising model.[11] Inside the coexistence region the disappearance of these droplets is accompanied by a pronounced maximum in the specific heat. Similar peaks were also observed in three dimensions.[12] However, rigorous results[6, 7, 9, 10] show that for the infinite two-dimensional lattice this transition takes place at the coexistence line. The same conclusion may be drawn from a rather simple and physically appealing argument which we will briefly discuss in the next section when dealing with the stability of three-dimensional droplets. One may therefore ask how to interpret these specific heat peaks in the light of what is known about this line.

As a thorough investigation of the caloric curve should shed new light on this problem, we studied the two- and the three-dimensional IMFM using the histogram method presented in the previous section. Two-dimensional square lattices with $N = L^2$ spins and three-dimensional simple cubic lattices with $N = L^3$ spins, both with full periodic boundary conditions, were simulated. The system sizes ranged from $L = 100$ to $L = 900$ in two dimensions and from $L = 10$ to $L = 80$ in three dimensions.

Figure 1 shows the computed microcanonical caloric curve e versus $1/\beta^*$ for the two-dimensional system at the fixed magnetization density $m_0 = M_0/N = 0.92$ for different system sizes. Here, β^* is the microcanonical inverse temperature defined in Eq. (2.9), whereas e is the intensive energy E/N. We emphasize again that the Gaussian smoothing procedure (see Section 2) used in this plot only reduces the unavoidable statistical errors. All the features discussed in the following are clearly visible in our original, unsmoothed, high-quality data.

Inspection of Fig. 1 reveals a completely different behavior of the system for small and large system sizes. For not too large systems (line (a)

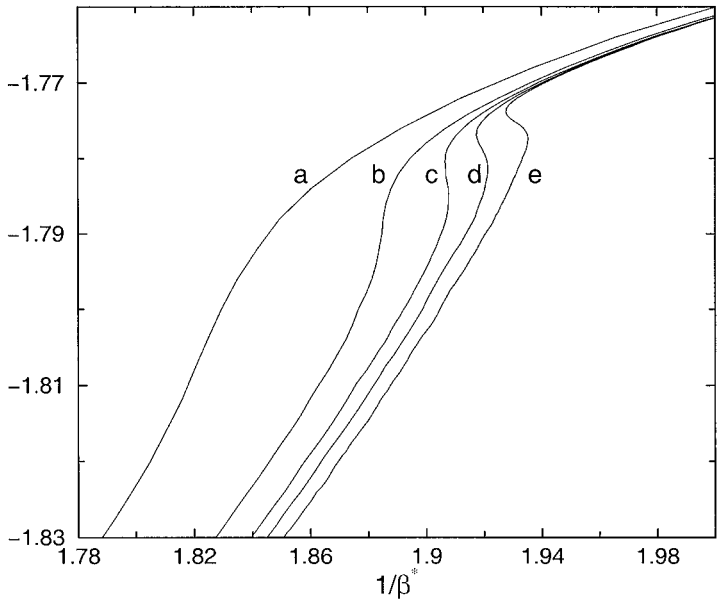

Fig. 1. Microcanonical caloric curves of the two-dimensional Ising model at the fixed magnetization $m_0 = 0.92$ for different system sizes: (a) $L = 100$, (b) $L = 200$, (c) $L = 300$, (d) $L = 400$, and (e) $L = 600$.

in Fig. 1) the caloric curve is monovalued, showing no indications of a possible phase transition. Increasing L leads first to a steepening of the curve (line (b)). After a threshold value has been passed, the monovaluedness is lost and the characteristic S-shape of a first order phase transition in finite systems[17] is observed (lines (c), (d), and (e)). This backbending of the caloric curve is associated with a segment of positive curvature of the entropy and leads to a negative microcanonical specific heat, see Eq. (2.11). Remarkably, large system sizes are needed in order to exhibit the S-shaped microcanonical caloric curve as the threshold value is around $L = 250$. Usually, in first order phase transitions, this characteristic behavior is already encountered for a small number of spins.[18] It is worth mentioning that the canonical caloric curve does not show this backbending for any system size.[17] One should further note that the same systematics have been observed, as a function of the number of atoms, in the theoretical study of the solid-liquid transition in Lennard–Jones clusters.[19]

The convex intruder, where the low- and the high-temperature phases coexist, is shown in Fig. 2 for two different system sizes. Here, the quantity $N(s - \beta_t e)$ is plotted as a function of the intensive energy. s is the microcanonical entropy $s(e, m_0) = N^{-1} \ln g(e, m_0)$ whereas the transition temperature

β_t^{-1} is obtained by the double tangent construction: On the major part of the energy axis $s(e)$ is a concave function of e. There the tangents of $s(e)$ lie completely above $s(e)$, in the convex part any tangent intersects $s(e)$. Between the two cases there is one tangent which touches $s(e)$ at the two points with the energies e_1 and e_2. This is the double tangent which determines the transition temperature β_t^{-1} and the finite system latent heat[17, 20] Δe at the same time:

$$\beta_t = \frac{s(e_2) - s(e_1)}{e_2 - e_1} \tag{3.1}$$

and

$$\Delta e = e_2 - e_1. \tag{3.2}$$

Note that the curves in Fig. 2 are raw, unsmoothed curves, demonstrating the good quality of our data.

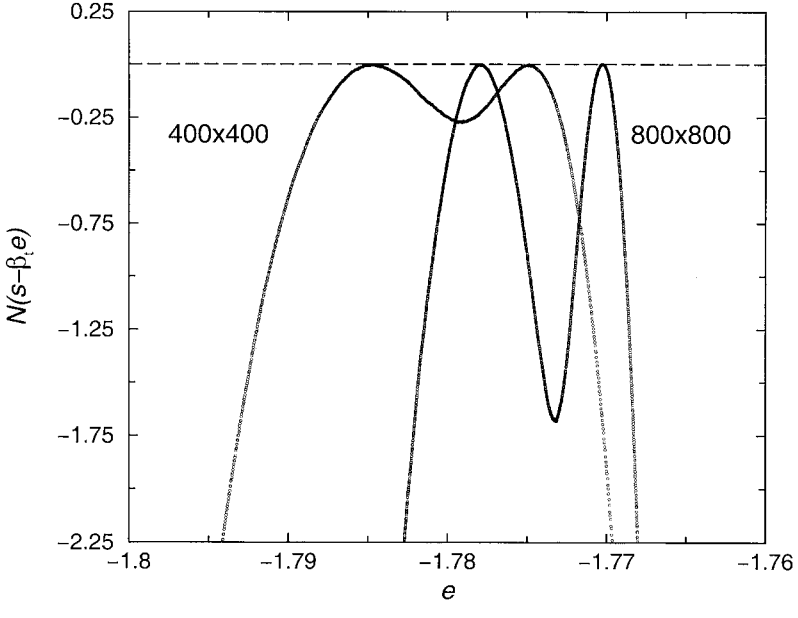

Fig. 2. The function $N(s-\beta_t e)$ versus the inverse energy e for the two-dimensional Ising model at constant magnetization $m_0 = 0.92$ for two different system sizes. We show the unsmoothed data, thus demonstrating their high quality.

From the finite-size scaling theory for first order phase transitions[21–24] it follows that the energies e_1 and e_2 should tend to their bulk values linearly in L^{-1}, whereas their difference, i.e., the latent heat (see Eq. (3.2)) must approach a constant value if the transition is really discontinuous. Furthermore, the asymptotic behavior of the transition temperature β_t^{-1} should be proportional to L^{-2d} (d being the dimensionality of the lattice),[22, 23] whereas the depth of the minimum of the function $s-\beta_t e$ should vanish as L^{-1}. In the present case, however, the situation is more complicated: The asymptotic behavior seems to be encountered only for the largest systems considered (difficulties in observing the asymptotic behaviour in first order phase transitions have also been reported in other systems[25]). As an example, Fig. 3 shows the evolution of the energies e_1 and e_2 as a function of L^{-1}. For systems with less than 800^2 spins, the energies e_1 and e_2 do not vary linearly in L^{-1}. The distance between these two energies, i.e., the latent heat, first increases, reaches a maximum for a system with about 400^2 spins, then decreases until, for $L = 800$, a linear dependency seems to prevail. Larger system sizes, which are beyond our present computer facilities, are needed to affirm unambiguously that the asymptotic regime has been reached.

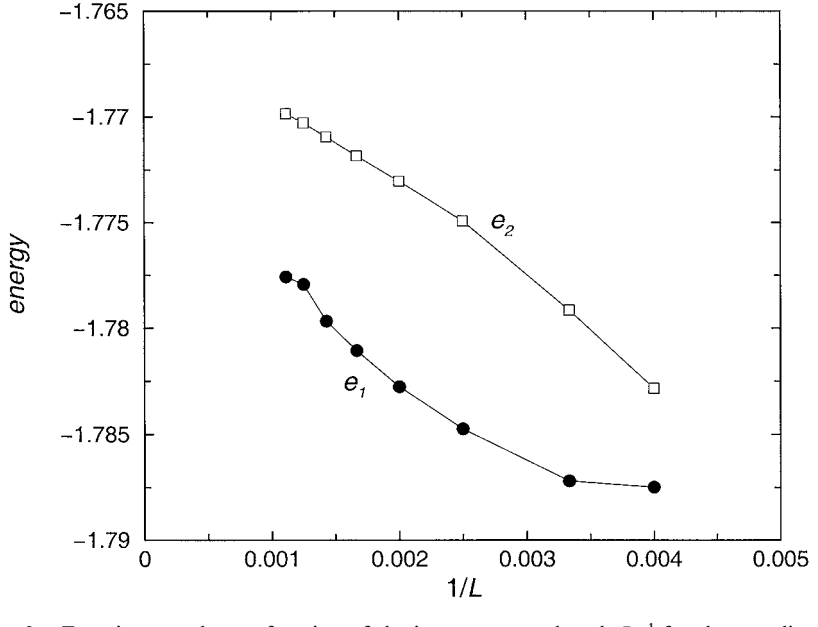

Fig. 3. Energies e_1 and e_2 as function of the inverse system length L^{-1} for the two-dimensional Ising model with $m_0 = 0.92$. The difference $e_2 - e_1$ is the latent heat. Error bars are smaller than the symbol sizes.

Turning now to the three-dimensional case, we show in Fig. 4 the microcanonical caloric curve for the fixed magnetization density $m_0 = 0.568$ as a function of the linear size L of the system. The same systematic behavior as in two dimensions is observed. Around 50^3 spins are needed in order to observe the typical S-shape of a continuous transition. Figure 5 shows the caloric curve of systems with $L = 60$ and different values of the fixed magnetization. At higher magnetizations, the phase transition takes place at lower values of the microcanonical temperature $1/\beta^*$, as would have been expected from the shape of the coexistence line. Remarkably, the discontinuous character of the transition is, at a given system size, much more pronounced at larger values of the magnetization. For small magnetization, see line (f) in Fig. 5, the caloric curve for $L = 60$ is monovalued and does not present the backbending. Clearly, larger system sizes have to be simulated when the magnetization is decreased in order to observe the characteristics of a possible first order phase transition. This may be related to the fact that along the coexistence line the correlation length increases with decreasing magnetization, diverging finally at the critical point.

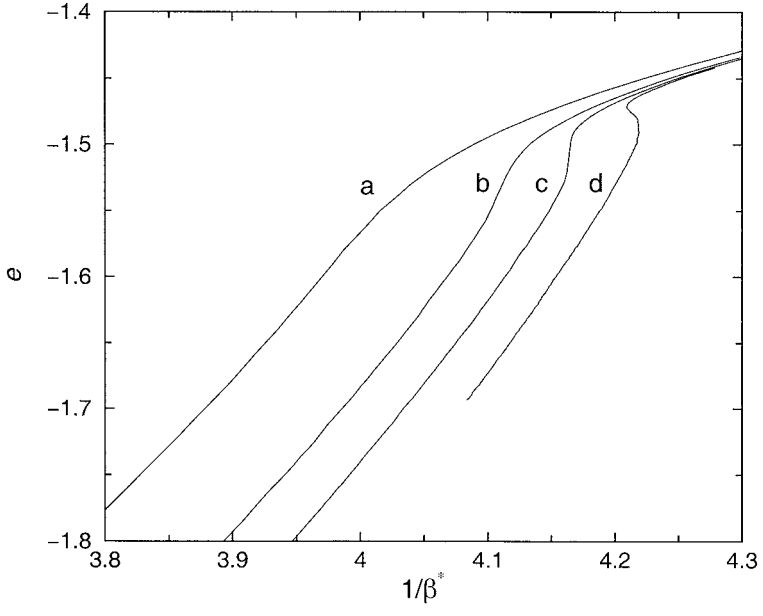

Fig. 4. Microcanonical caloric curves of the three-dimensional Ising model at the constant magnetization $m_0 = 0.568$ for system sizes (a) $L = 20$, (b) $L = 30$, (c) $L = 40$, and (d) $L = 60$.

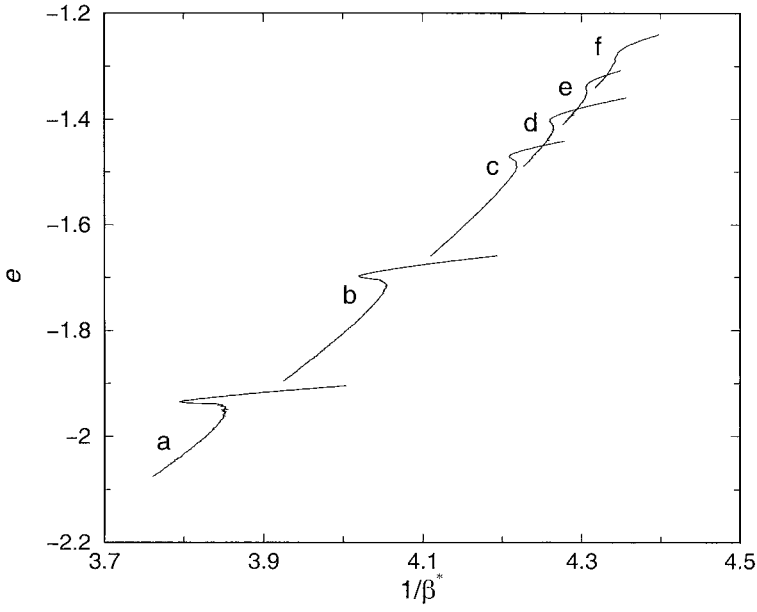

Fig. 5. Microcanonical caloric curves obtained for a system with 60^3 spins for various fixed magnetizations: (a) $m_0 = 0.75$, (b) $m_0 = 0.66725$, (c) $m_0 = 0.568$, (d) $m_0 = 0.531$, (e) $m_0 = 0.492$, and (f) $m_0 = 0.45075$.

Our data for large system sizes are in accordance with conclusions drawn from the expected topology of the entropy in finite systems.[14] With the two-phase region excepted, the entropy is a concave function of the energy e and the magnetization density m, i.e., both the principal curvatures are negative. Inside the two-phase region of a finite system one of the principal curvatures becomes positive. Inspection of the eigenvectors of the curvature matrix reveals that the convex intruder should then be encountered when crossing the coexistence line at fixed magnetization, as is observed in our simulations of large systems. On the other hand, our simulations of small systems show that the backbending of the caloric curve is not visible for system sizes L smaller than some characteristic, magnetization dependent, length which may be related to the correlation length. Thus, our results explain why data from simulations of three-dimensional moderate sized systems (up to 40^3 spins) at low magnetizations were erroneously interpreted as evidence for a continuous phase transition[12] and they refute the recent claim that at constant volume in the corresponding lattice gas model the microcanonical caloric curve does not possess the typical S-shape.[26]

4. DROPLETS IN THREE DIMENSIONS

In this section, we will discuss the influence of finite-size effects on the thermal stability, at fixed magnetization, of three-dimensional macroscopic droplets of minority spins inside the coexistence region of the Ising model.[27, 28] To be more specific, we will assume a positive fixed magnetization m_0, so that the $\sigma = -1$ spins are the minority spins. By the term "macroscopic droplet" we denote an extensive cluster of connected minority spins with an average of $\langle N_c \rangle$ spins whose size scales with the system size N. A corresponding study in two dimensions[11] has recently shown that these droplets loose their extensivity at a cluster transition which is expected to take place at the coexistence line in the thermodynamic limit. In fact, one may argue that, in the infinite system, the mean magnetization density in the droplet has the same absolute value as in the rest of the system. As a consequence, the following expression for the reduced droplet size $n_c = \langle N_c \rangle / N_-$ (N_- being the total number of $\sigma = -1$ spins) in the thermodynamic limit is easily derived[11]:

$$n_c(T) = (1+m_{sp})(m_{sp}-m_0)/(2m_{sp}(1-m_0)) \tag{4.1}$$

where m_{sp} is the spontaneous magnetization at the temperature T. It follows from this expression, in accordance with rigorous results, that the extensive droplet vanishes in the infinite system at the coexistence line. Note that no assumption on the dimensionality of the system was made for the derivation of Eq. (4.1). In finite systems, this cluster transition is accompanied by a pronounced peak in the specific heat (as obtained from energy fluctuations), thus showing its connection to the transition discussed in the previous section.

The assumption of equal absolute values of the magnetizations inside and outside the droplet is not expected to hold at high temperatures in finite systems. In fact, due to the Gibbs–Thomson effect, which describes the effect of curved interfaces at equilibrium,[29, 30] the fraction of minority spins forming the droplet at fixed magnetization m_0 should be reduced in finite systems as compared to the infinite system, thus leading to a decrease of the reduced droplet size n_c as well as to a shift of the cluster transition temperature to lower values. This is exactly what has been observed in simulations in two dimensions.[11]

Figures 6 and 7 show the temperature dependent droplet size $n_c(L)$ for different system sizes L in the three dimensional case for two different fixed magnetizations $m_0 = 0.75$ and $m_0 = 0.568$. This data were obtained with a nonlocal spin-exchange algorithm,[16] specially conceived for the study of equilibrium crystal shapes, which we adapted to the

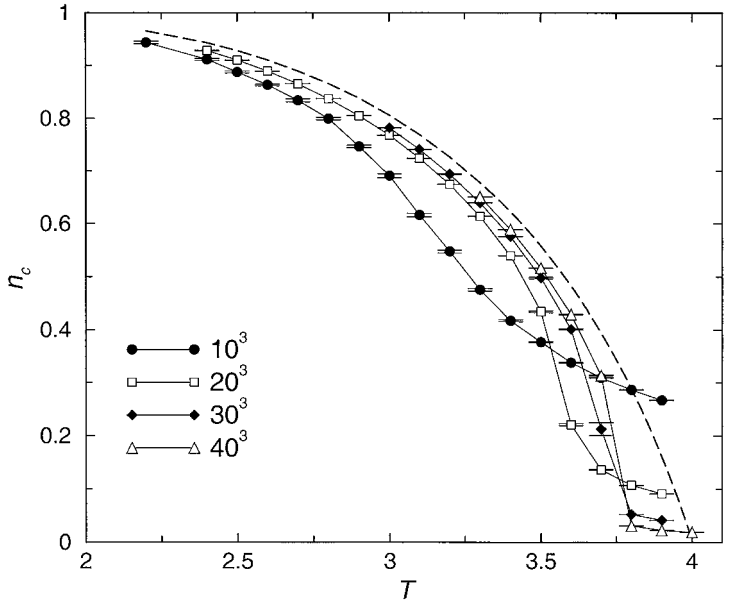

Fig. 6. Reduced droplet size n_c as function of temperature for different lattice sizes as obtained from Monte Carlo simulations of the three-dimensional IMFM with $m_0 = 0.75$. Here and in the following error bars are obtained by averaging over at least 10 runs with different random numbers. The dashed line is the theoretical prediction (4.1) for the infinite system.

three-dimensional IMFM. The dashed lines are obtained from Eq. (4.1). For the spontaneous magnetization $m_{sp}(T)$ we used the expression given in ref. 31.

Consider first the case $m_0 = 0.75$ (Fig. 6). For this value of the fixed magnetization, the reduced droplet size $n_c(L)$ for finite L is shifted to lower values when compared to the theoretical prediction (Eq. (4.1)), but it clearly approaches the theoretical curve when L is increased. Furthermore, the cluster transition temperature, given by the turning point of $n_c(L)$, is reduced for decreasing system sizes. These results are readily understood when invoking the Gibbs–Thomson effect and are similar to the finite size dependences observed in two dimensions. Note that for increasing system sizes, the decrease in $n_c(L)$ evolves from a slow smooth decrease for small systems to a rapid, almost discontinuous, change for larger systems, in accordance with the systematics discussed in the previous section.

It has been proven rigorously[6, 9] that at fixed magnetization density m_0 in a d-dimensional hypercube with L^d sites (L very large, $L \to \infty$) one big droplet is observed as long as

$$m_{sp}(T) - m_0 \gg L^{-\frac{d}{d+1}} \tag{4.2}$$

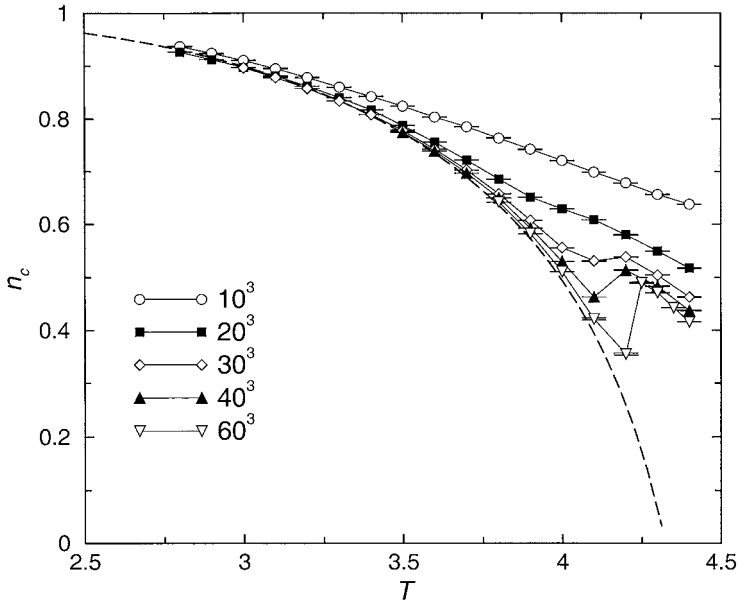

Fig. 7. The same as in Fig. 6, but now for the conserved magnetization $m_0 = 0.568$.

whereas many small droplets with sizes at most as large as $\ln L$ are encountered if

$$m_{sp}(T) - m_0 \ll L^{-\frac{d}{d+1}}. \tag{4.3}$$

Setting $m_{sp}(T) - m_0 = L^{-\frac{d}{d+1}}$ one may derive for a given m_0 and a given L a typical temperature separating these two regimes. These temperatures coincide rather well with the transition temperatures defined as the turning points of the reduced droplet sizes, see Fig. 6, even if the rigorous proof only holds in the limit $L \to \infty$. The same is true for droplets in the two-dimensional Ising model, see Fig. 2 in ref. 11.

For $m_0 = 0.568$ (Fig. 7), the finite system sizes manifest themselves in a completely different and unexpected way. The reduced droplet size now approaches the theoretical curve from above, i.e., the fraction of minus spins forming the droplet is larger in finite systems than compared to what is expected from the assumptions leading to Eq. (4.1). This behavior is in marked contrast to the Gibbs–Thomson effect.

Our explanation of this behavior is based on percolation theory.[32] Recall that in the three-dimensional Ising model, the percolation temperature T_p for the type of clusters we are considering (i.e., clusters of minority

spins connected by a nearest-neighbor bond) is located below the critical temperature T_c.[33, 34] Therefore, for temperatures larger than T_p, an infinite cluster of minority spins, which is not a compact object but a fractal, is encountered at the coexistence line in the infinite system. In the present case, the crossing of the line $m_0 = 0.568$ and the coexistence line is located slightly above the percolation temperature. It is then not surprising to observe that the extensive droplet contains a larger fraction of minority spins than predicted under the assumptions (involving implicitly compact objects) leading to Eq. (4.1). In fact, above the percolation temperature, Eq. (4.1) should not be valid any more. The data in Fig. 7 show that in finite systems even at temperatures below T_p the droplet has a tendency to be formed by an increased number of minority spins. These conclusions are supported by results for the reduced size of the largest cluster formed by minus spins in the two-dimensional IMFM at magnetization $m_0 = 0$. Note that for the two-dimensional Ising model the critical temperature and the percolation temperature coincide. In the simulations of the two-dimensional IMFM with $m_0 = 0$ larger clusters than theoretically predicted are also observed, in accordance with the fact that the $m_0 = 0$ line crosses the line of spontaneous magnetization at the critical (percolation) temperature, whereas for all other investigated values of the fixed magnetizations $m_0 \neq 0$ a decrease of the reduced droplet size is encountered when compared to the theoretical line (4.1).[11]

Coming back to Fig. 7, we observe further for large system sizes a discontinuous jump in $n_c(L)$. This jump is related to the transition encountered when the coexistence line is crossed, as discussed in Section 3. In contrast to the case of larger values of m_0 (see Fig. 6), where the discontinuous change is at best guessed for large system sizes, the discontinuity in the droplet size is here clearly observed. This is a consequence of the largeness of the droplets of minority spins when crossing the coexistence line in the vicinity of the percolation temperature. Note that discontinuous changes are also observed in the second moments of the cluster size distributions.

5. CONCLUSIONS

Despite of the fact that the Ising model has been studied extensively since more than 70 years and despite of its possible applications in solid state and nuclear physics, there are still some open questions regarding its behaviour at constant magnetization m_0 in finite systems. In three dimensions it may serve as a model system for the solid to gas transition of a fixed number of particles in a given volume or for the fragmentation of nuclear matter. The two-dimensional Ising model is used to describe the transition from a cluster of adatoms on a surface to a gaslike behaviour.

We have performed a series of MC calculations in two and three dimensions for several values of m_0 and for a wide range of system sizes. For large systems the data hint at a possible discontinuous phase transition with a well resolved latent heat. The discontinuity disappears for smaller systems and it diminishes when m_0 is reduced.

It is well known that the canonical ensemble is ill prepared for a distinction between continuous and discontinuous phase transitions.[35] All singularities are smeared out. It is therefore essential that the data, although obtained in normal canonical simulations, be analyzed microcanonically.

There a possible discontinuous transition is clearly visible in finite systems as a convex intruder in the entropy as a function of the energy (see Fig. 2). In a canonical analysis one averages over a great number of energy channels leading to a loss of information which is especially bad in the two phase region between the two maxima of $s(e)-\beta_t e$. In the vicinity of the transition temperature $T_t = 1/\beta_t$ the partition function is dominiated by one or the other of the two maxima.

When the energy is plotted versus the microcanonically defined temperature, the convex intruder manifests itself as an S-shape in the caloric equation. This is shown in Figs. 1, 4, and 5.

There is no discontinuity present for small systems—it develops only for astonishingly large systems. Despite of the very large system sizes which have been studied, we are not able to assert that the scaling region has already been reached, but larger systems surpass our present computer capacities. Figure 5 shows that, for a given size, the discontinuous character diminishes when m_0 is reduced. On the basis of the present data we cannot decide if for very large systems there is a discontinuity for all finite m_0 or if it disappears before the limit $m_0 = 0$ is reached. For sufficiently large systems and for sufficiently large values of m_0 a discontinuity is observed both in two and three dimensions.

These results also explain why the decay of the macroscopic droplets of minority spins with rising energy inside the coexistence region of finite systems is signalled by a peak in the specific heat. In fact, these droplets loose their extensivity at the coexistence line when crossing this line at temperatures below the percolation temperature. Above the percolation temperature, the macroscopic Ising clusters percolate the system, the crossing of the coexistence line showing up as discontinuous jumps in the cluster properties.

ACKNOWLEDGEMENTS

We would like to thank D. H. E. Gross, M. Henkel, H. Müller-Krumbhaar, J. Richert, W. Selke, and Y. Velenik for useful discussions and D. d'Enterria for bringing ref. 2 to our attention.

REFERENCES

1. B. McCoy and T. T. Wu, *The Two-Dimensional Ising model* (Harvard University Press, Cambridge, 1973).
2. J. Richert and P. Wagner, Microscopic model approaches to fragmentation of nuclei and phase transitions in nuclear matter, *Phys. Rep.*, in print and preprint nucl-th/0009023.
3. K. Binder, Theory of first-order phase transitions, *Rep. Prog. Phys.* **50**:783 (1987).
4. A. J. Bray, Theory of phase-ordering kinetics, *Adv. in Phys.* **43**:357 (1994).
5. C. Rottman and M. Wortis, Statistical mechanics of equilibrium crystal shapes: Interfacial phase diagrams and phase transitions, *Phys. Rep.* **103**: 59 (1984).
6. R. L. Dobrushin, R. Kotecký, and S. Shlosman, *The Wulff construction: A global shape from local interactions*, AMS, Translations of Mathematical Monographs, Vol. 104 (Providence, Rhode Island, 1992).
7. T. Bodineau, D. Ioffe, and Y. Velenik, Rigorous probabilistic analysis of equilibrium crystal shapes, *J. Math. Phys.* **41**:1033 (2000), and references therein.
8. T. Müller and W. Selke, Stability and diffusion of surface clusters, *Eur. Phys. J. B* **10**:549 (1999).
9. R. L. Dobrushin and S. B. Shlosman, Large and moderate deviations in the Ising model, *Advances in Soviet Mathematics* **20**:91 (1994).
10. D. Ioffe and R. Schonmann, Dobrushin–Kotecký–Shlosman theory up to the critical temperature, *Comm. Math. Phys.* **199**:117 (1998).
11. M. Pleimling and W. Selke, Droplets in the coexistence region of the two-dimensional Ising model, *J. Phys. A: Math. Gen.* **33**:L199 (2000).
12. J. M. Carmona, J. Richert, and A. Tarancón, A model for nuclear matter fragmentation: phase diagram and cluster distributions, *Nucl. Phys. A* **643**:115 (1998).
13. H. W. J. Blöte, J. R. Heringa, and M. M. Tsypin, Three-dimensional Ising model in the fixed-magnetization ensemble: A Monte Carlo study, *Phys. Rev. E* **62**:77 (2000).
14. D. H. E. Gross and E. V. Votyakov, Phase transitions in "small" systems, *Eur. Phys. J. B* **15**:115 (2000).
15. A. M. Ferrenberg and R. H. Swendsen, New Monte Carlo method for studying phase transitions, *Phys. Rev. Lett.* **61**:2635 (1988).
16. G. T. Barkema, M. E. J. Newman, and M. Breeman, Model for the shapes of islands and pits on (111) surfaces of fcc metals, *Phys. Rev. B* **50**:7946 (1994).
17. A. Hüller, First order phase transitions in the canonical and the microcanonical ensemble, *Z. Phys. B* **93**:401 (1994).
18. M. Schmidt, MC-Simulation of the 3D, $q=3$ Potts model, *Z. Phys. B* **95**:327 (1994).
19. P. Labastie and R. L. Whetten, Statistical thermodynamics of the cluster solid-liquid transition, *Phys. Rev. Lett.* **65**:1567 (1990).
20. D. H. E. Gross, *Microcanonical Thermodynamics: Phase Transitions in "Small" Systems*, Lecture Notes in Physics, Vol. 66 (World Scientific, Singapore, 2001).
21. J. Lee and J. M. Kosterlitz, Finite-size scaling and Monte Carlo simulations of first-order phase transitions, *Phys. Rev. B* **43**:3265 (1991).
22. C. Borgs and R. Kotecký, A rigorous theory of finite-size scaling at first-order phase transitions, *J. Stat. Phys.* **61**:79 (1990).
23. C. Borgs and R. Kotecký, Finite-size effects at asymmetric first-order phase transitions, *Phys. Rev. Lett.* **68**:1734 (1992).
24. C. Borgs, R. Kotecký, and S. Miracle-Solé, Finite-size scaling for the Potts models, *J. Stat. Phys.* **62**:529 (1991).
25. A. Stemmer and A. Hüller, Monte Carlo simulation of type-1 fcc Ising antiferromagnets, *Phys. Rev. B* **58**:887 (1998).

26. F. Gulminelli, P. Chomaz, and V. Duflot, Abnormal kinetic-energy fluctuations and critical behaviors in the microcanonical lattice gas model, *Europhys. Lett.* **50**:434 (2000).
27. T. Bodineau, The Wulff construction in three and more dimensions, *Commun. Math. Phys.* **207**:197 (1999).
28. R. Cerf and A. Pisztora, On the Wulff crystal in the Ising model, *Ann. Probab.* **28**:945 (2000).
29. K. Binder and M. H. Kalos, "Critical clusters" in a supersaturated vapor: Theory and Monte Carlo simulation, *J. Stat. Phys.* **22**:363 (1980).
30. B. Krishnamachari, J. McLean, B. Cooper, and J. Sethna, Gibbs–Thomson formula for small island sizes: Corrections for high vapor densities, *Phys. Rev. B* **54**:8899 (1996).
31. A. L. Talapov and H. W. J. Blöte, The magnetization of the 3D Ising model, *J. Phys. A: Math. Gen.* **29**:5727 (1996).
32. D. Stauffer and A. Aharony, *Introduction to Percolation Theory* (Harvard University Press, Cambridge, 1994).
33. H. Müller-Krumbhaar, Percolation in a lattice system with particle interaction, *Phys. Lett.* **50A**:27 (1974).
34. A. Coniglio, C. R. Nappi, F. Peruggi, and L. Russo, Percolation points and critical point in the Ising model, *J. Phys. A: Math. Gen.* **10**:205 (1977).
35. K. Binder (ed.), *The Monte Carlo Method in Condensed Matter Physics* (Springer, Heidelberg, 1992).